NASA Technical Memorandum 81958

Preliminary Feasibility Analysis of a Pressure Modulator Radiometer for Remote Sensing of Tropospheric Constituents

Harry D. Orr III and Pamela L. Rarig

APRIL 1981

NASA

NASA Technical Memorandum 81958

Preliminary Feasibility Analysis of a Pressure Modulator Radiometer for Remote Sensing of Tropospheric Constituents

Harry D. Orr III
Langley Research Center
Hampton, Virginia

Pamela L. Rarig
Systems and Applied Sciences Corporation
Hampton, Virginia

National Aeronautics
and Space Administration

**Scientific and Technical
Information Branch**

1981

SUMMARY

A preliminary analysis has been performed of the feasibility of using a pressure modulator radiometer (PMR) in a nadir-viewing mode as a tropospheric pollutant sensor. For the purposes of this study, the pressure modulator drive was assumed to have the thermal and mechanical characteristics of the instrument flown in the Stratospheric and Mesopheric Sounder experiment aboard the Nimbus 7 satellite. The sensitivity of the instrument to changes in the mean volumetric mixing ratio of carbon monoxide in the atmosphere was studied as a function of modulator cell length and mean pressure. The preliminary study used a model atmosphere having a pressure-temperature profile corresponding to a mid-latitude summer model, but with carbon monoxide, at a mean volumetric mixing ratio of 0.1 ppm, as the only infrared-active gas. The integrated signal from the instrument was calculated over the passband from 2075 cm^{-1} to 2215 cm^{-1} for gas cell lengths of 0.5, 1.0, 2.0, and 3.0 cm and mean cell pressures of 16.7, 33.3, 66.7, 133, and 267 mb (1 mbar = 0.1 kPa). Performance was evaluated on the basis of signal-to-noise ratio (SNR) for a 10-percent change ΔQ in the mean volumetric mixing ratio of carbon monoxide. The relative sensitivity to concentration changes confined to narrow altitude layers was also studied. The maximum SNR(ΔQ) of about 33.5 occurred at a cell length of approximately 1 cm and a mean cell pressure of approximately 66.7 mbar. For this case, the sensitivity was maximum for mixing ratio changes in the vicinity of 10 km and fell to half its maximum value at about 4 km. The results indicated that a sensitivity which peaks at a lower altitude (e.g., 7 km) for better overall or multilevel tropospheric measurements could be obtained with a cell length of 2 to 3 cm and a mean cell pressure of about 267 mbar. For the pressure modulator drive of the Nimbus 7 design, these cell parameters would produce a signal-to-noise ratio of 8 to 11 for a 10-percent change in mean CO mixing ratio. This ratio might be improved by up to a factor of 7 through modifications to the drive control circuitry. It was concluded that further improvement would require a pressure modulator drive having a larger swept volume and producing higher compression ratios at higher mean cell pressures than the current design.

INTRODUCTION

The pressure modulator radiometer (PMR), a passive infrared correlation radiometer, is being considered for monitoring tropospheric trace gases in the nadir-viewing mode from a high-altitude aircraft or satellite platform. This paper presents preliminary results of a theoretical study of the PMR as a tropospheric gas monitor.

In the gas correlation technique, a sample of the gas of interest is used to modulate the spectrum of incoming atmospheric radiation. The modulation can be achieved either by using multiple optical paths, each containing a sample of the gas at a known temperature and pressure, or by changing the pressure (and temperature) of the gas in a single optical path. The first technique is

employed in such experiments as the Selective Chopper Radiometer (SCR) and the Measurement of Air Pollution from Satellites (MAPS). (See refs. 1 and 2.) The second approach is represented by the PMR (ref. 3), in which an electromechanically driven piston causes the pressure (and temperature) of the gas in a sample cell to oscillate.

Both of the techniques outlined above share with other passive remote sensing systems the advantages of relatively low weight, volume, and power requirements. In addition, the gas correlation technique accepts a relatively broad spectral input (on the order of 100 cm^{-1}) while maintaining a high degree of spectral selectivity. Thus the difference in radiation transmitted through two cells or a single cell at two different pressures is directly related to the mean volumetric mixing ratio of the gas of interest in the atmosphere.

Correct interpretation of the data from a gas correlation device requires precise control of any conditions within the instrument which influence the transmission of atmospheric radiation through the optical path or paths. In the first technique (SCR or MAPS), the pressure and temperature of the gas in the cells must be known accurately and any relative change in the transmissivity of optical components must be accounted for in either the signal processing circuitry or the data reduction algorithms. In the second technique (PMR), changes in the components of the single optical path have no effect on the difference in transmitted radiation; moreover, the pressures and temperatures can be monitored through the frequency of the device, since the piston and gas cell comprise a resonant system. An additional potential advantage of the single optical path in the PMR technique is the possiblility of using cells in series. For example, one cell might contain a reference gas such a N_2O or $^{13}CO_2$, whose concentration in the atmosphere is well-known, stable, and uniformly mixed, to monitor changes in atmospheric temperature and correct the inferred pollutant mean mixing ratio. This capability gives the PMR a potentially significant advantage over other tropospheric constituent sensors whose measurements are typically quite dependent on assumptions or external sources of information about the temperature profile. Quantitative data, such as signal-to-noise ratios, and vertical sensitivity distributions are required to assess the potential improvements in tropospheric monitoring capability.

SYMBOLS

A_d area of detector, cm^2

A_o area of optics, cm^2

D^* detectivity of detector, $cm\text{-}Hz^{1/2}/W$

L radiance at detector, $W/(cm^2\text{-}sr\text{-}cm^{-1})$

N Planck radiation function, at a wave number for the mean pressure and temperature of a given atmospheric layer, $W/(cm^2\text{-}sr\text{-}cm^{-1})$

p average pressure of an atmospheric layer, mbar (1 mbar = 0.1 kPa)

p_o	sea-level pressure, mbar
q	volumetric mixing ratio of gas in an individual atmospheric layer
Q	mean volumetric mixing ratio of a uniformly mixed species
r	compression ratio
R	upwelling radiance at top of atmosphere at a wave number, $W/(cm^2\text{-}sr\text{-}cm^{-1})$
S_{NB}	narrow-band signal, instrument-modulated atmospheric radiance integrated over wave number, $W/(cm^2\text{-}sr)$
S_{WB}	wide-band signal, average atmospheric radiance transmitted by instrument integrated over wave number, $W/(cm^2\text{-}sr)$
SNR	signal-to-noise ratio
T	average temperature of an atmospheric layer, K
V_c	volume of pressure modulator cell, cm^3
V_o	volume of dead space above piston at top of stroke, cm^3
V_s	volume swept by piston, cm^3
W	pseudo-weighting-function of an atmospheric layer
Δf	instrument electronic bandwidth, Hz
ΔQ	change in uniform mixing ratio, 10 percent in this study
ϵ	emissivity of the surface
ν	wave number, cm^{-1}
τ	transmissivity of an atmospheric layer at a wave number
τ_o	overall transmissivity of optics
τ_{WB}	transmissivity of wide-band filter at a wave number
Ω	solid angle, sr

Subscripts:

c1	conditions in instrument cell at maximum pressure
c2	conditions in instrument cell at minimum pressure
D1	conditions at detector at maximum cell pressure

D2 conditions at detector at minimum cell pressure

k,ℓ,m average conditions in kth, ℓth, and mth atmospheric layer

APPROACH

The preliminary analysis of instrument performance reported in this study required four steps. First, the upwelling infrared radiation from the Earth and atmosphere is calculated for the passband of the instrument. Second, the signal modulation characteristics of the PMR are computed for a range of instrument parameters. Third, the net signal produced by the response of the instrument to the upwelling radiation is determined for each PMR configuration. Fourth, the sensitivity of the signal to changes in the average pollutant concentration and to changes in the concentration at particular altitudes is calculated for the given set of instrument parameters.

Atmospheric Radiation

The upwelling infrared radiation from the surface of the Earth and active constituents in the atmosphere is calculated using a radiative transfer computer program called SMART (refs. 4 and 5). This program treats the atmosphere as a series of plane, parallel, homogeneous layers, each described by pressure, temperature, thickness, and volumetric mixing ratios of one or more gaseous constituents. For this purpose the atmosphere is assumed to consist of 15 layers as shown in table I. The pressure, temperature, and number density of each layer are derived from the "mid-latitude summer" model of the atmosphere (ref. 6). The thicknesses of the layers are selected to represent approximately equal optical paths. The transmission spectrum of each layer is calculated at uniform wave-number increments (0.01 cm^{-1} in the present study) from a library of spectral line data (ref. 7). The program accounts for the temperature dependence of the strength of each spectral line and the pressure and temperature dependence of the width of each line.

The pollutant of interest for this analysis is carbon monoxide (CO). The infrared band used is centered at 2145 cm^{-1}; the passband used is defined by a rectangular broadband filter which transmits radiation from 2075 cm^{-1} to 2215 cm^{-1}. In this spectral region there are several other active atmospheric species which could interfere with detection of CO: carbon dioxide, water vapor, ozone, nitrous oxide, and carbonyl sulfide. A complete experiment feasibility analysis would include a study of these potential sources of error and techniques for minimizing their effects; however, these species are not included in this preliminary analysis because of the computational cost of treating the large number of spectral lines involved. Hence, CO at a uniform mixing ratio of 0.1 ppm is assumed to be the only infrared-active species present. The surface of the Earth is assumed to radiate as a gray body with an emissivity of 0.86 and a temperature of 294 K. In this initial study, no contribution from reflected solar radiation is included. Thus, the conditions represent a night-

time measurement over an average land surface. The effects of atmospheric radiation emitted in the downward direction and reflected upward by the surface are also ignored.

The upwelling radiance at the top of the atmosphere at wave number ν is computed from the expression,

$$R_\nu = \sum_{\ell=0}^{15} N_\ell(\nu,\tau_\ell)[1 - \tau_\ell(\nu,p_\ell,T_\ell)] \prod_{j=\ell+1}^{15} \tau_j(\nu,p_\ell,T_\ell) \qquad (1)$$

where N_ℓ is the Planck function and τ_ℓ is the transmission of layer ℓ at wave number ν (note that the 0th term in the summation refers to the surface contribution with τ_0 defined as $1 - \varepsilon$ where ε is the emissivity of the surface). Also, τ_j is defined to be 1 for $j > 15$.

Since the gas filter correlation technique depends on the convolution of the upwelling atmospheric spectrum with that of the gas in the instrument cell, it is important that the effects of pressure and temperature on individual line shapes be accurately simulated, both in the atmosphere and in the instrument. Hence an accurate knowledge of the pressure-temperature cycle of the instrument gas cell is needed. In addition, accurate spectral line data are required.

For the mid-latitude summer model of the atmosphere containing only a uniformly mixed CO concentration of 0.1 ppm, the contribution of each layer (but not of the surface) to the total upwelling radiance at the top of the atmosphere, i.e., $\int R_\nu \tau_{WB}\, d\nu$, is shown in figure 1. In the troposphere, the upwelling radiance is strongly influenced by the atmospheric temperature structure. For this reason, the temperature-sensing potential of the PMR, mentioned in the Introduction, is of great interest.

Instrument Modulation Characteristics

The principal features of the pressure modulator radiometer are shown in figure 2. A cell containing a sample of the gas of interest (CO) is located, as shown, in the optical train in front of the radiation detector. An electrically driven piston causes the pressure in the cell to oscillate. The frequency of the oscillation depends on the mean cell pressure and ranges from 30 Hz to 90 Hz. These pressure (and temperature) oscillations change the shapes of the vibration-rotation spectral lines of the gas and hence the transmittance of the cell. If the radiance signals detected at the maximum and minimum cell pressures are subtracted, the effect is approximately the same as if a series of doubly peaked filters, centered at each spectral line of the sample gas, were imposed on the incoming radiation. This process is illustrated in figure 3 for one typical line. It is important to note that the variation of pressure in the cell is accompanied by a change in temperature of the gas.

Thus, a portion of the change in signal observed at the detector is produced by a change in radiation emitted by the gas in the cell.

Accurate radiometric modeling of the PMR requires knowledge of the relations among piston position, cell pressure, and gas temperature. These relations depend on the change of gas temperature with pressure, the rate of flow of gas between the volume above the piston and the cell, leakage between the volume above the piston and that below it, heat conduction between the gas and the walls of the PM drive and cell, and electromechanical features of the piston. (See fig. 2(b).)

For the current study, the cell pressure and gas temperature as a function of piston position are obtained by means of a computer program furnished by personnel at the Department of Atmospheric Physics of Oxford University, Oxford, U.K. The program calculates, at small increments in piston position, the flow of gas (assumed to be Poiseuille (ref. 8)) between various volumes, the initial temperature changes of the gas (assumed to be adiabatic) in various volumes, and the temperature relaxation caused by heat conduction between the gas and the walls over the small time step associated with the incremental piston motion. The maximum extent of piston motion is determined by the parameters describing the electromechanical drive (i.e., drive coil power, helical spring constant, and piston mass) and the differential pressure acting on the piston. For any given mean cell pressure, the PM drive constitutes a resonant system. The computation continues until a stable oscillatory mode is established. The effective relation between pressure and volume in the gas cell is found to be polytropic (ref. 9), i.e., intermediate between isothermal and adiabatic.

For the analysis reported here, the pressure and temperature as a function of piston position were obtained for several cell lengths of the same diameter. The appropriate volumes were used in the computation, while the times for temperature relaxation were assumed to depend primarily on cell diameter and were therefore held constant. Also computed was the compression ratio r, a convenient parameter to characterize the amount of pressure modulation. The compression ratio is defined by

$$r = 1 + \frac{V_S}{V_O + V_C}$$

where V_S is the volume swept by the piston, V_O is the dead space above the piston at the top of its stroke (not including the volume of the cell), and V_C is the volume of the cell.

Signal Detection

The radiance from the atmosphere transmitted by the gas cell and the radiance emitted by the gas in the cell are combined to yield the total radiance L at the detector. For the maximum pressure (1) and minimum pressure (2), these quantities are

$$\left.\begin{aligned} L_{D1} &= \int\{R_\nu\,\tau_{c1}(\nu,p_{c1},T_{c1}) + N_\nu(T_{c1})[1 - \tau_{c1}(\nu,p_{c1},T_{c1})]\}\tau_{WB}(\nu)\,d\nu \\ L_{D2} &= \int\{R_\nu\,\tau_{c2}(\nu,p_{c2},T_{c2}) + N_\nu(T_{c2})[1 - \tau_{c2}(\nu,p_{c2},T_{c2})]\}\tau_{WB}(\nu)\,d\nu \end{aligned}\right\} \quad (2)$$

From these quantities, two types of signals are formed:

$$S_{NB} = L_{D1} - L_{D2} \quad (3)$$

and

$$S_{WB} = \frac{L_{D1} + L_{D2}}{2} \quad (4)$$

As a convenient shorthand reference, the quantity S_{NB} is designated the "narrow-band" signal since it exhibits the specific correlation of the narrow spectral lines of the gas in the cell with the atmospheric spectrum. The quantity S_{WB} is designated the "wide-band" signal since it represents an average of the incoming radiation.

Instrument Sensitivity

The overall objective of a tropospheric monitoring instrument is to detect variations in time and space of the concentration of a particular trace constituent. This detection process has two important aspects. One is the sensitivity of the method to changes in the mean volumetric mixing ratio; the other is the relative sensitivity to particular vertical regions of the troposphere.

By analogy with the analysis of other infrared systems (ref. 10, pp. 19-3 - 19-13), a figure of merit to describe the first aspect of instrument performance is the noise equivalent mixing ratio change, that is, the change in mixing ratio that produces a signal-to-noise ratio (SNR) of 1. For the presentation of results in this study, it is convenient to use the reciprocal of this quantity: SNR evaluated for a mixing ratio change of 10 percent, written as SNR(ΔQ). This quantity is computed from the expression,

$$SNR(\Delta Q) = \frac{\partial S_{NB}}{\partial Q}(\Delta Q/NER) \quad (5)$$

where NER is the noise equivalent radiance of the radiometer, given by (ref. 10, pp. 11-17)

$$NER = \frac{\sqrt{A_d}\ \sqrt{\Delta f}}{D^* A_o \Omega \tau_o} \tag{6}$$

To evaluate the NER, values for the variables in equation (6) were assumed which would occur in a typical radiometer design (see table II).

Differentiation of equation (3) with respect to the average CO mixing ratio Q gives

$$\frac{\partial S_{NB}}{\partial Q} = \int \left\{ \sum_{\ell=0}^{15} N_\ell \left[(1 - \tau_\ell) \left(\sum_{k=\ell+1}^{15} \frac{1}{\tau_k} \frac{\partial \tau_k}{\partial Q} \right) - \frac{\partial \tau_\ell}{\partial Q} \right] \left(\prod_{j=\ell+1}^{15} \tau_j \right) \right\} (\tau_{c2} - \tau_{c1}) \tau_{WB}\, d\nu \tag{7}$$

For a single uniformly mixed species of volumetric mixing ratio Q the partial derivative of τ_k can be replaced by

$$\frac{\partial \tau_k}{\partial Q} = \tau_k \frac{\ln \tau_k}{Q} \tag{8}$$

for computation.

The second aspect of the instrument capability is the relative response of the instrument to changes in the CO concentration in a single layer while concentrations in all other layers are unchanged; it thus reveals to which vertical region of the atmosphere a particular instrument configuration is most sensitive. This concept of sensitivity is different from that of "weighting function" as used in temperature sounding. The upwelling radiance at the top of the atmosphere can be expressed in a general form as

$$R_\nu = \int_0^\infty N_\nu[T(y)] \frac{d\tau_\nu(y)}{dy}\, dy \tag{9}$$

where $y = -\ln p$, p is the atmospheric pressure, T(y) is the temperature at the altitude represented by y, and $\tau(y)$ is the transmission between this altitude and the top of the atmosphere. Equation (1) is a numerical approximation to this expression for an atmosphere divided into homogeneous layers and also includes the contribution from the surface. In the analysis of radiometric sounding, the quantity $\frac{d\tau_\nu(y)}{dy}$ is designated the "weighting function" (ref. 11). For a broadband radiometer an integral over the passband is performed. The

integral over y is normalized to one. By comparing equations (1) and (9), one can infer a corresponding weighting function for the mth homogenous layer of the atmosphere

$$W_m = \int \left[(1 - \tau_m) \prod_{j=m+1}^{15} \tau_j \right] (\tau_{c2} - \tau_{c1}) \tau_{WB} \, d\nu \qquad (10)$$

The typical effects of different mean cell pressures on this function are illustrated in figure 4 for a cell length of 1.0 cm. However, because of the strong thermal structure of the troposphere, a distinction must be made in the case of constituent sensing between the contribution of a given layer to the signal (i.e., radiance) and the information about species concentration contained in that contribution. The figure does illustrate the fact that as the mean pressure is increased, the gas filter tends to correlate with portions of the atmospheric radiance arising from lower altitudes. In other words, the modulated cell transmittance perferentially passes radiance occurring further from the centers of CO lines in the atmospheric spectrum.

While the profile information represented by the single-layer sensitivity cannot be obtained experimentally from any single measurement by a PMR of the type considered in this study, this quantity can provide a useful tool. For example, several PMR's could be used simultaneously, each designed to be most sensitive to concentration changes at a different altitude.

Since the primary interest is in the relative sensitivity to changes in various layers, this function is normalized to unity at its maximum value. Differentiation of the right side of equation (3) with respect to q_m, the mixing ratio of the target species in the mth layer, gives the single-layer sensitivity for the mth layer:

$$\frac{\partial S_{NB}}{\partial q_m} = \int \left\{ \left[\sum_{\ell=0}^{m-1} N_\ell (1 - \tau_\ell) \left(\frac{1}{\tau_m} \right) \prod_{j=\ell+1}^{15} \tau_j - N_m \prod_{j=m+1}^{15} \tau_j \right] \left(\frac{\partial \tau_m}{\partial q_m} \right) (\tau_{c2} - \tau_{c1}) \right\} \tau_{WB} \, d\nu \qquad (11)$$

RESULTS AND DISCUSSION

Instrument Operation Characteristics

For the results presented in this report, the dimensions (table III) assumed for the PM drive are those of the drive designed for flight aboard the Nimbus 7 satellite on the SAMS (Stratospheric and Mesospheric Sounder) experiment (ref. 12). The dimensions of the gas cells used in the simulations are derived from a design by Langley Research Center personnel for laboratory studies of the PMR. The dimensions of the cells studied and the results of the gas dynamics computer program are summarized in table IV for the four cell lengths and five mean pressures used. The typical relationships between pressure and piston position and between pressure and temperature are shown in

figures 5 and 6 for a 1-cm cell with mean cell pressure of 66.7 mbar. These plots illustrate the phase differences between pressure and temperature induced by gas flow and heat conduction. It should be noted that the computed compression ratio is less than the potential maximum that would be obtained if the piston traveled through its maximum stroke. This effect is a feature of the drive circuit electronics, which are designed to restrict the driving force in order to maintain symmetrical motion of the piston about its equilibrium position.

Variation of Signal-to-Noise Ratio With Instrument Parameters

Figure 7 shows the variation of SNR(ΔQ) with mean cell pressure for cell lengths of 0.5, 1.0, 2.0, and 3.0 cm, for the mid-latitude summer model of the atmosphere containing only CO. The SNR(ΔQ) peaks between mean cell pressures of approximately 60 and 130 mbar. The same data are plotted in figure 8 as a function of cell length for the mean cell pressures of 16.7, 33.3, 66.7, 133, and 267 mbar used in this study. Viewed in this manner, the data indicate that for mean pressures between 60 and 130 mbar, the SNR(ΔQ) reaches a maximum near a cell length of 1 cm. The highest maximum value of SNR(ΔQ) was 33.5 at a mean cell pressure of 66.7 mbar.

The SNR(ΔQ) depends on the shape and magnitude of the modulation function; this function in turn depends in a somewhat complicated way on both the widths of the lines and the degree of absorption by the gas in the cell. The widths of these lines are determined by the pressures and temperatures at the extrema of the PM drive cycle, while the amount of absorption varies with cell length.

Consider a 1-cm cell at 66.7 mbar as a reference point. For lower mean pressures, the modulation fuctions are narrower and transmit portions of the atmosphere spectrum arising from higher, cooler altitudes; the greater magnitude of the modulation signal produced by the somewhat higher compression ratio at the lower cell pressures does not completely compensate for the effect of this lower source strength. At higher mean cell pressures, the modulation functions are broader and transmit atmospheric radiation from lower, warmer altitudes but the overall decrease in the amount of modulation because of lower compression ratios produces a net reduction in the SNR(ΔQ).

At a fixed mean cell pressure, the behavior of the SNR(ΔQ) depends on the degree to which the absorption lines in the cell are saturated. Low saturation of the lines in the shorter cells produces narrower modulation functions; in the longer cells, saturation begins to occur, broadening the modulation function and transmitting the stronger signals from lower altitudes. Ultimately, the accompanying decrease in compression ratio forces the SNR(ΔQ) to fall. For a mean cell pressure of 267 mbar, the absorption lines are so broad that the decreasing compression ratio dominates the SNR(ΔQ) behavior over the entire range of cell length.

Variation of Vertical Sensitivity Distribution

With Instrument Parameters

Figure 9 shows the variation of the vertical sensitivity distribution (VSD) with mean cell pressure and cell length. The curves are cubic spline fits through points at the mean altitude of each layer. It is interesting to note that the sensitivity to concentration changes in the lowest one or two layers may be opposite in sign to the sensitivity at higher altitudes. The physical reason behind this situation can be seen by examining equation (11) for the first layer:

$$\frac{\partial S_{NB}}{\partial q_1} = \int (N_0 \epsilon - N_1) \left(\prod_{j=2}^{15} \tau_j \right) \left(\frac{\partial \tau_1}{\partial q_1} \right) (\tau_{c2} - \tau_{c1}) \tau_{WB} \, d\nu \qquad (12)$$

The sign of this term evidently depends on the relative magnitudes of the radiances from the surface and the first layer and the emissivity ϵ of the surface.

Figure 9 also demonstrates the distinction to be made between the upwelling atmospheric radiance, which originates principally in the lower layers of the troposphere (see fig. 1), and the species concentration information contained in that radiance. The usefulness of the PMR technique depends on the interpretation of an observed change in signal in terms of a change in species concentration. If a change in species concentration in a particular altitude range produces no change in the observed signal, then the radiance from that region contains no information about species concentration from the viewpoint of the PMR. However, a change in the observed signal may be produced by a change in the average temperature of the molecules in that region. Further, equation (11) can be factored into the form,

$$\frac{\partial S_{NB}}{\partial q_m} = \int \left\{ \left[\sum_{\ell=0}^{m-1} N_\ell (1 - \tau_\ell) \prod_{j=\ell+1}^{m-1} \tau_j - N_m \right] \left(\prod_{j=m+1}^{15} \tau_j \right) \left(\frac{\partial \tau_m}{\partial q_m} \right) \right\} (\tau_{c2} - \tau_{c1}) \tau_{WB} \, d\nu \qquad (13)$$

The summation within the first set of brackets represents the upwelling radiance at the bottom of the mth layer. Thus, if this quantity is very nearly equal to the Planck blackbody radiance N_m of the mth layer, the change in narrowband signal produced by any change in the pollutant concentration in layer m is difficult to observe because the value of the integral approaches zero. There is also the possibility of a situation in which N_m is large enough in comparison with values at lower levels, e.g., an atmospheric temperature inversion, that the sign of the change in S_{NB} would be opposite to that expected for a normal temperature profile.

Figure 10 shows the altitude variation of the maximum and lower half-maximum of the VSD as a function of mean cell pressure for each of the cell lengths considered. One design consideration which can be deduced from these

data is that doubling mean cell pressure is approximately equivalent to quadrupling the cell length in terms of lowering the altitude at which the maxima and half-maxima of the VSD occur.

Note that at the conditions for which SNR(ΔQ) is maximum (1-cm cell at 66.7 mbar), the maximum of the VSD in figure 10 occurs at 10.25 km and the half-maximum at about 4 km. For measurement of average tropospheric CO burden, a VSD peak nearer the middle of the troposphere is desirable. For a 2- to 3-cm cell at a mean pressure of 667 mbar, the maximum of the VSD occurs at 7 km. However, at these cell conditions, the values of SNR(ΔQ) are between 8 and 11 (fig. 8).

It can also be seen in figure 10 that the resolution of the VSD (i.e., the difference in altitude between the maximum and the lower half-maximum) decreases (improves) with increases in both mean cell pressure and cell length, ranging from about 8 km for the 0.5-cm cell at 16.7 mbar to 4 km for the 3.0-cm cell at 267 mbar.

Finally, for all cell lengths, the location of the half-maximum appears to approach a limit of about 2.7 km at a mean cell pressure of 267 mbar.

Relation Between Signal-to-Noise Ratio and Compression Ratio

In figure 11, the SNR(ΔQ) is plotted as a function of compression ratio. From these data it can be seen that for mean cell pressures up to 66.7 mbar, the SNR(ΔQ) depends much more strongly on mean cell pressure than on compression ratio. Conversely, for higher pressures, SNR(ΔQ) is a strong function of compression ratio. This situation reflects the fact that at higher mean cell pressures, small changes in pressure have little effect on the vertical region of the atmosphere sampled, i.e., the source strength (see fig. 10); however, changes in mean cell pressure do have a significant effect on the extent of variation in transmission of the cell.

It is of interest to estimate the SNR(ΔQ) which could be achieved with the Nimbus 7 type PM drive if the electronic drive circuitry were modified to allow the maximum possible volume (see table IV) to be swept by the piston at a mean cell pressure of 267 mbar. Extrapolating the data in figure 11 for this pressure to a compression ratio of 1.26 gives a SNR(ΔQ) between 50 and 60 (improvement by a factor of 7); any greater improvement in the SNR(ΔQ) would require a PM drive design having a larger swept volume.

CONCLUSION

The purpose of this paper is to present results of a preliminary feasibility analysis of using the pressure modulator radiometer (PMR) concept as a nadir-viewing tropospheric gas sensor. The particular instrument studied is not designed for tropospheric applications, but the variation of the key parameters, cell length, and mean cell pressure, within the limited performance

envelope available, suggests the potential capability of the concept for making tropospheric measurements.

In particular, for a given PM drive design, the signal-to-noise ratio (SNR) for a given change in pollutant burden ΔQ and the vertical sensitivity distribution (VSD) to single-layer concentration changes are uniquely determined by the choice of PM cell length and mean cell pressure which in turn determine the compression ratio. For the Nimbus 7 type PM drive modeled in this analysis and a mid-latitude summer model of the atmosphere with a mean volumetric CO mixing ratio of 0.1 ppm, the SNR(ΔQ) reaches a maximum of about 33 for a cell length of 1 cm and mean cell pressure of 66.7 mbar; these parameters determine a VSD which peaks at about 10.25 km. For measurements of average tropospheric CO burden it is desirable that this peak occur at a lower altitude, nearer the middle of the troposphere. As an example, the cell parameters required to achieve a VSD peak at about 7 km, a cell length of 2 to 3 cm and mean cell pressure of 267 mbar, yield SNR(ΔQ) values between approximately 8 and 11. Although some improvement (e.g., a factor of 7) may be obtained by modifying the electronic control of the Nimbus 7 PM drive, significantly higher values of the SNR(ΔQ) would require a drive capable of a larger swept volume. Beyond the requirement for a more powerful PM drive, future analysis should include studies of interference from water vapor and other species. The effects on data retrieval of uncertainties in temperature profile should be examined together with the feasibility of reducing these effects by use of a temperature reference gas. In addition, the influence of variations in ground temperature and emissivity should be assessed. An analysis should be made of potential advantages of alternate passbands such as the 2.35-μm region, where the dominant reflected solar radiation might permit greater sensitivity at lower altitudes.

Langley Research Center
National Aeronautics and Space Administration
Hampton, VA 23665
March 17, 1981

REFERENCES

1. Abel, P. G.; Ellis, P. J.; Houghton, J. T.; Peckham, G.; Rodgers, C. D.; Smith, S. D.; and Williamson, E. J.: Remote Sounding of Atmospheric Temperature From Satellites. II. The Selective Chopper Radiometer for Nimbus D. Proc. R. Soc. London, ser. A, vol. 320, no. 1540, Nov. 24, 1970, pp. 35-55.

2. Hesketh, W. D.; Reichle, H. G.; Massey, W. A.; Ward, T. V.; and Zwick, H. H.: A Gas Filter Correlation Instrument for Atmospheric Trace Constituent Monitoring. Remote Sensing of Earth Resources, Volume V, F. Shahrokhi, ed., Univ. of Tennessee, Space Inst., c.1977, pp. 527-556.

3. Taylor, F. W.; Houghton, J. T.; Peskett, G. D.; Rodgers, C. D.; and Williamson, E. J.: Radiometer for Remote Sounding of the Upper Atmosphere. Appl. Optics, vol. 11, no. 1, Jan. 1972, pp. 135-141.

4. Casas, Joseph C.; and Campbell, Shirley A.: A Modular Radiative Transfer Program for Gas Filter Correlation Radiometry. NASA CR-2895, 1977.

5. Rarig, Pamela L.: Adaptation and Optimization of a Line-by-Line Radiative Transfer Program for the STAR-100 (STARSMART). NASA CR-159238, 1980.

6. McClatchey, R. A.; Fenn, R. W.; Selby, J. E. A.; Volz, F. E.; and Garing, J. S.: Optical Properties of the Atmosphere (Third Edition). AFCRL-72-0497, U.S. Air Force, Aug. 24, 1972. (Available from DTIC as AD 753 075.)

7. Rothman, L. S.: AFGL Atmospheric Absorption Line Parameters Compilation: 1980 Version. Appl. Opt., vol. 20, no. 5, Mar. 1, 1981, pp. 791-795.

8. White, Frank M.: Viscous Fluid Flow. McGraw-Hill, Inc., c.1974, pp. 121-125.

9. Crawford, Franzo H.: Heat, Thermodynamics, and Statistical Physics. Harcourt, Brace & World, Inc., c.1963, pp. 135-137.

10. Wolfe, William L.; and Zissis, George J., eds.: The Infrared Handbook. Off. Naval Res., Dep. of the Navy, 1978, pp. 19-3 - 19-13.

11. Curtis, P. D.; Houghton, J. T.; Peskett, G. D.; and Rodgers, C. D.: Remote Sounding of Atmospheric Temperature From Satellites. V. The Pressure Modulator Radiometer for Nimbus F. Proc. R. Soc. London, ser. A, vol. 337, no. 1608, Mar. 5, 1974, pp. 135-150.

12. Drummond, J. R.; Houghton, J. T.; Peskett, G. D.; Rodgers, C. D.; Wale, M. J.; Whitney, J.; and Williamson, E. J.: The Stratospheric and Mesospheric Sounder on Nimbus 7. Philos. Trans. R. Soc. London, ser. A, vol. 296, no. 1418, Mar. 6, 1980, pp. 219-241.

TABLE I.- PHYSICAL PROPERTIES OF THE 15-LAYER

MID-LATITUDE SUMMER MODEL OF THE ATMOSPHERE

[Derived from ref. 6]

Layer	Thickness, km	Mean pressure, mbar	Mean temperature, K	Mean CO density, molecules/cm^3
1	0.60	973.3	292.9	2.41×10^{12}
2	.63	908.3	290.4	2.27
3	.68	840.8	287.3	2.12
4	.73	773.1	283.4	1.97
5	.78	706.5	278.9	1.84
6	.85	639.5	274.0	1.69
7	.93	572.2	268.7	1.54
8	1.03	504.7	262.8	1.39
9	1.16	437.8	256.2	1.23
10	1.33	369.8	247.9	1.08
11	1.57	302.3	238.6	.92
12	1.92	234.5	227.4	.75
13	2.58	166.3	216.6	.56
14	4.42	97.0	216.1	.33
15	80.79	5.6	227.3	.02

TABLE II.- VALUES OF PARAMETERS USED IN CALCULATION OF NOISE

EQUIVALENT RADIANCE (EQ. (6))

A_d	(area of detector), cm^2	0.04
A_o	(area of optics), cm^2	5.07
D*	(detectivity of detector), cm-$Hz^{1/2}$/W	8.0×10^{10}
Δf	(instrument electronic bandwidth), Hz	0.44
τ_o	(overall transmissivity of optics)	0.5
Ω	(instrument solid angle), sr	4.8×10^{-3}
NER	(noise equivalent radiance), W/(cm^2-sr)	1.36×10^{-10}

TABLE III.- PERTINENT DIMENSIONS AND GAS DYNAMIC CHARACTERISTICS OF PRESSURE MODULATOR DRIVE

Diameter of piston, cm	3.0
Volume above piston (includes one-half of volume of tube between drive and cell), cm^3	1.62
Volume below piston, cm^3	6.084
Volume below drive magnet, cm^3	12.67
Mass of moving parts, kg	0.1824
Volume rate of Poiseuille flow per unit pressure differential, $(cm^3/sec)/Pa$:	
1. Between volume above piston and cell	5.51
2. Between volumes above and below piston	1.70×10^{-3}
3. Between volumes below piston and below magnet	1.51×10^{-2}
Time constant for CO temperature relaxation:	
1. Cell, sec-cm^3/g	26.7
2. Volume above piston (as function of piston displacement X), sec-cm/g	$297(0.214 - X)^2$
3. Volume below piston	759
4. Volume below magnet	759
Spring constants:	
1. First order, N/cm	442.8
2. Third order, N/cm^3	1.440×10^7
Drive coil constants:	
1. Drive force constant, N/cm	1.0
2. Drive velocity constant, cm/sec	3.5
3. Drive offset constant, N/cm	10

TABLE IV.- DIMENSIONS AND OPERATING CHARACTERISTICS OF GAS CELLS

Length, cm	Volume, cm^3	Maximum compression ratio	Computed compression ratio	Mean pressure, mbar	Minimum pressure, p_{min}, mbar	Temperature at p_{min}, K	Maximum pressure, p_{max}, mbar	Temperature at p_{max}, K	Frequency, Hz
0.5	2.72	2.04	1.56	16.7	13.3	295.8	20.9	296.8	34.2
			1.54	33.3	26.8	294.7	41.7	299.5	41.5
			1.40	66.7	55.2	290.2	80.7	305.1	53.4
			1.21	133	118.1	288.0	150.4	305.7	73.2
			1.11	267	247.8	290.3	286.9	302.4	102.4
1.0	4.34	1.65	1.38	16.7	14.3	295.8	39.5	298.1	39.6
			1.37	33.3	28.6	295.0	39.5	298.1	39.6
			1.30	66.7	57.9	291.5	77.7	302.4	50.4
			1.17	133	120.6	289.4	147.5	303.8	68.0
			1.09	267	251.4	291.4	282.9	301.1	94.3
2.0	7.59	1.37	1.23	16.7	15.1	295.9	18.6	296.2	32.0
			1.22	33.3	30.2	295.3	37.2	297.1	37.7
			1.20	66.7	60.6	293.0	73.8	299.7	47.2
			1.12	133	124.1	291.2	143.6	301.4	62.8
			1.07	267	255.3	292.5	278.7	299.7	85.8
3.0	10.83	1.26	1.16	16.7	15.5	295.9	18.1	296.1	31.5
			1.16	33.3	31.0	295.5	36.2	296.7	36.8
			1.14	66.7	62.1	293.8	72.1	298.6	45.7
			1.10	133	126.0	292.2	141.5	300.1	60.1
			1.05	267	257.7	293.2	276.2	298.9	81.5

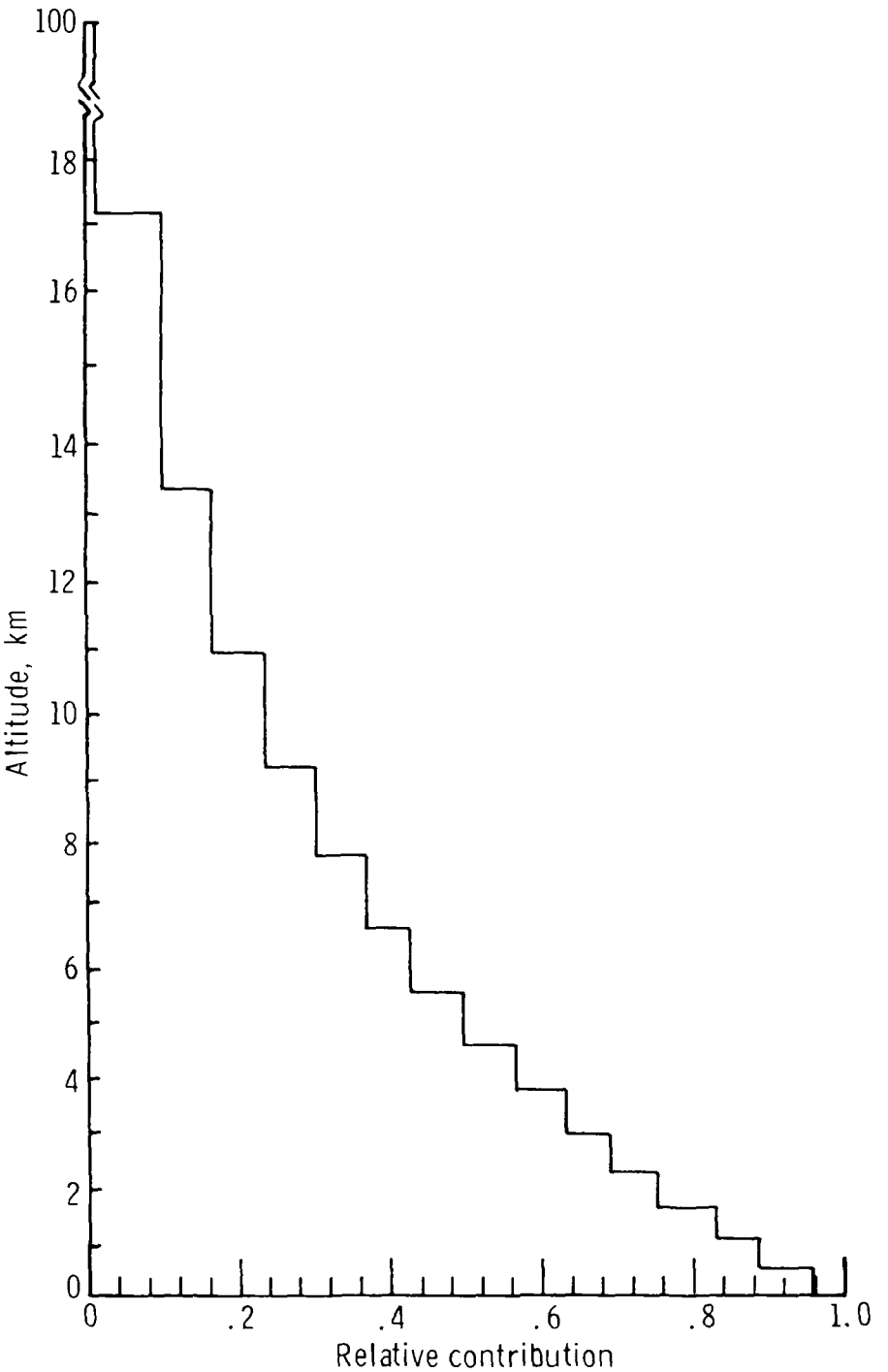

Figure 1.- Relative contribution of each layer of mid-latitude summer model, with CO the only infrared-active species, to total upwelling radiance as observed from the top of the atmosphere (uppermost layer extends from 17 to 100 km).

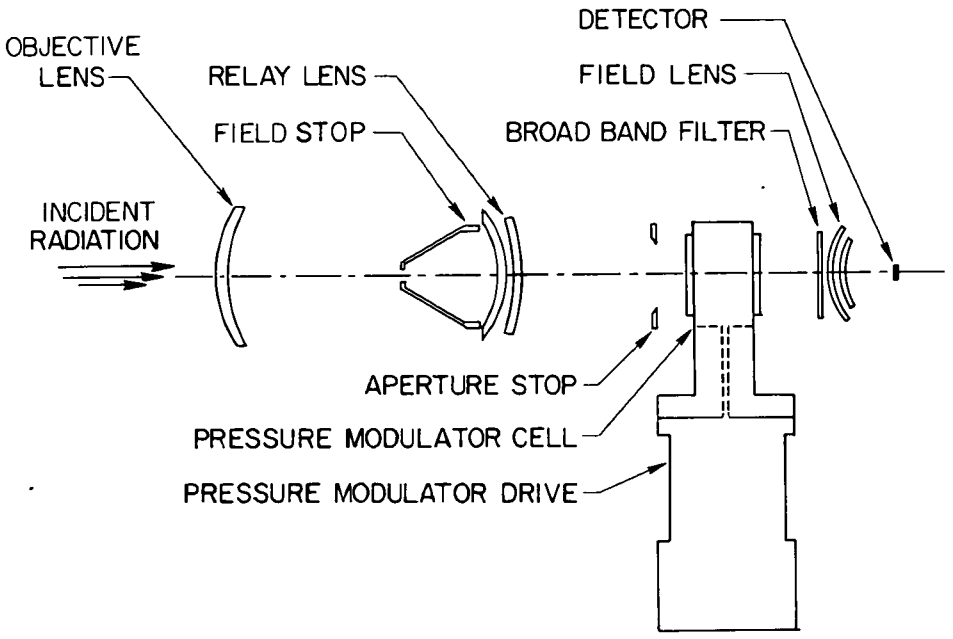

(a) Schematic of optics.

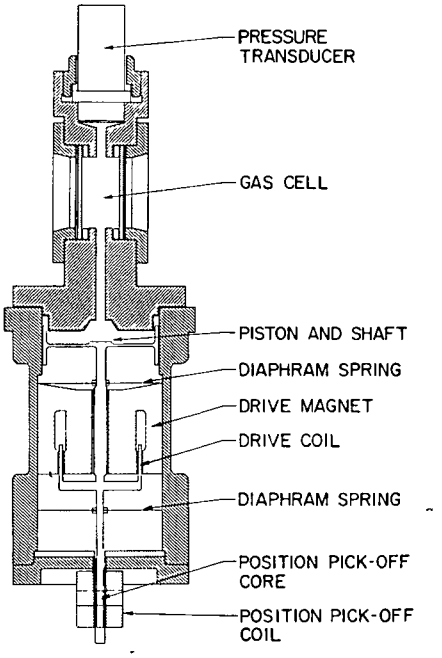

(b) Schematic of pressure modulator drive with experimental gas cell and pressure transducer.

Figure 2.- Pressure modulator radiometer.

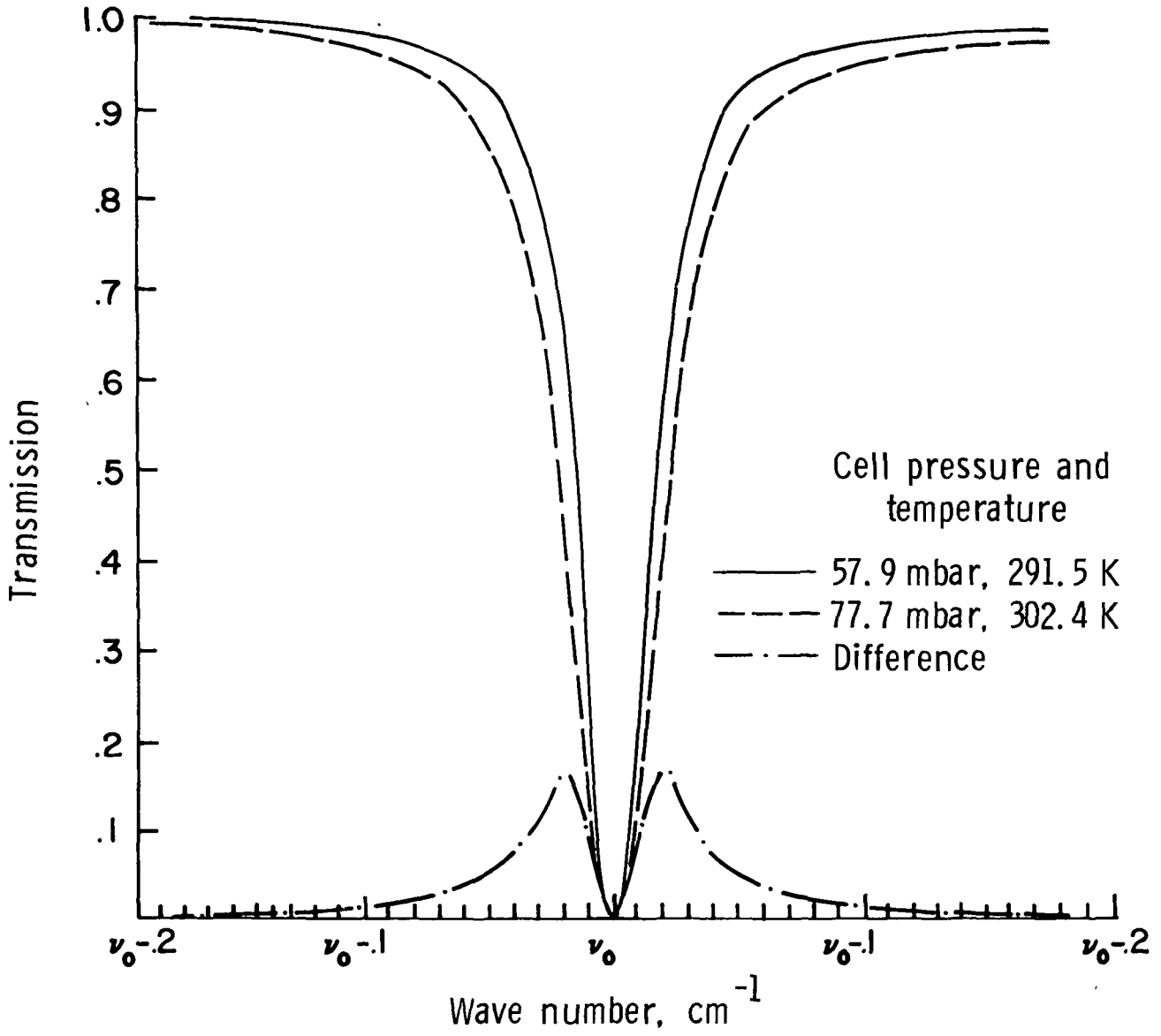

Figure 3.- Transmission spectra near a typical line center (with wave number ν_o) for two cell conditions and the difference representing pressure modulator gas filter function.

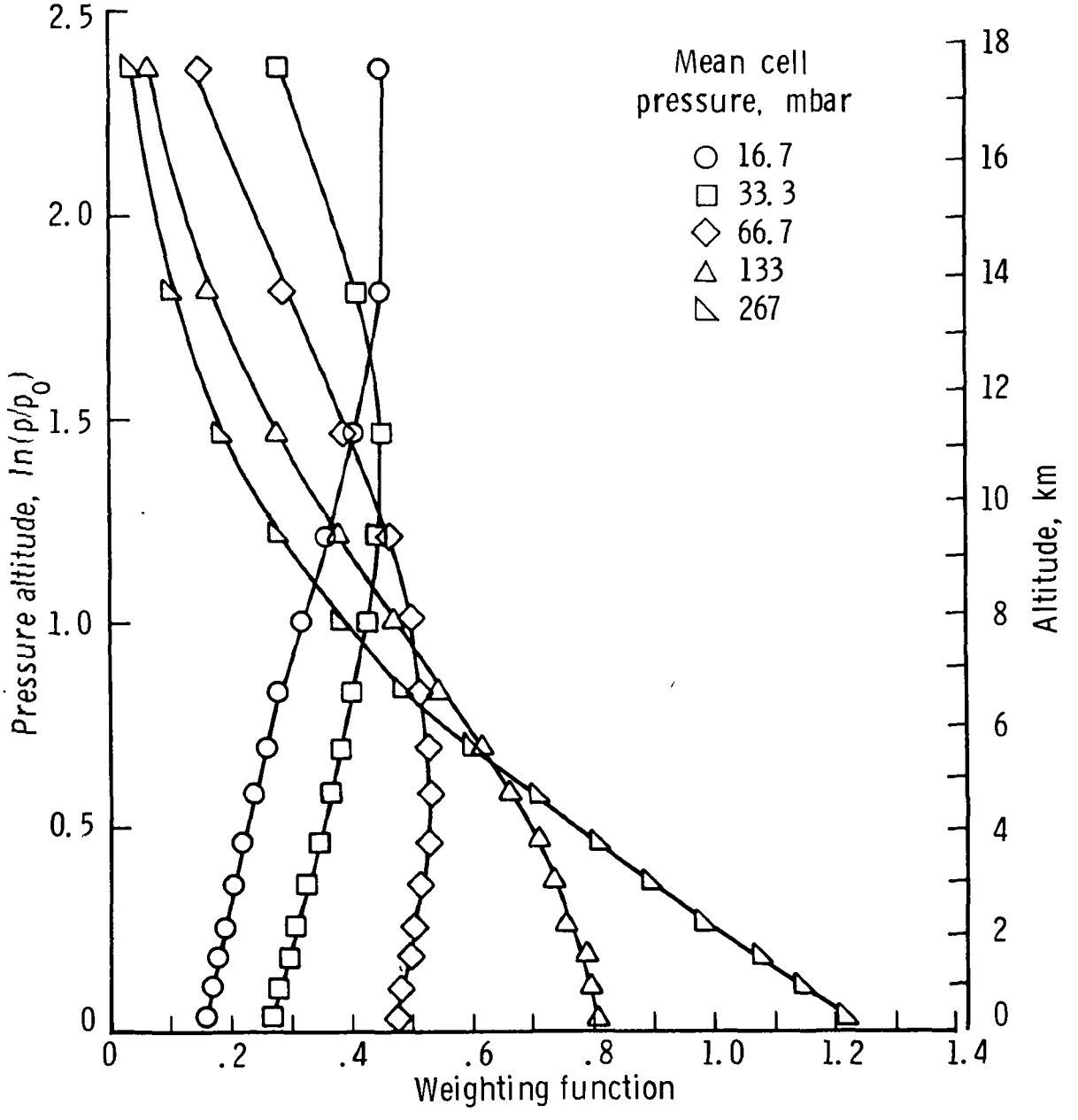

Figure 4.- Weighting function for mid-latitude summer model atmosphere, with CO the only infrared-active species, for a 1-cm cell at five mean cell pressures (see eq. (10)). Integral of each curve over altitude is normalized to 1.

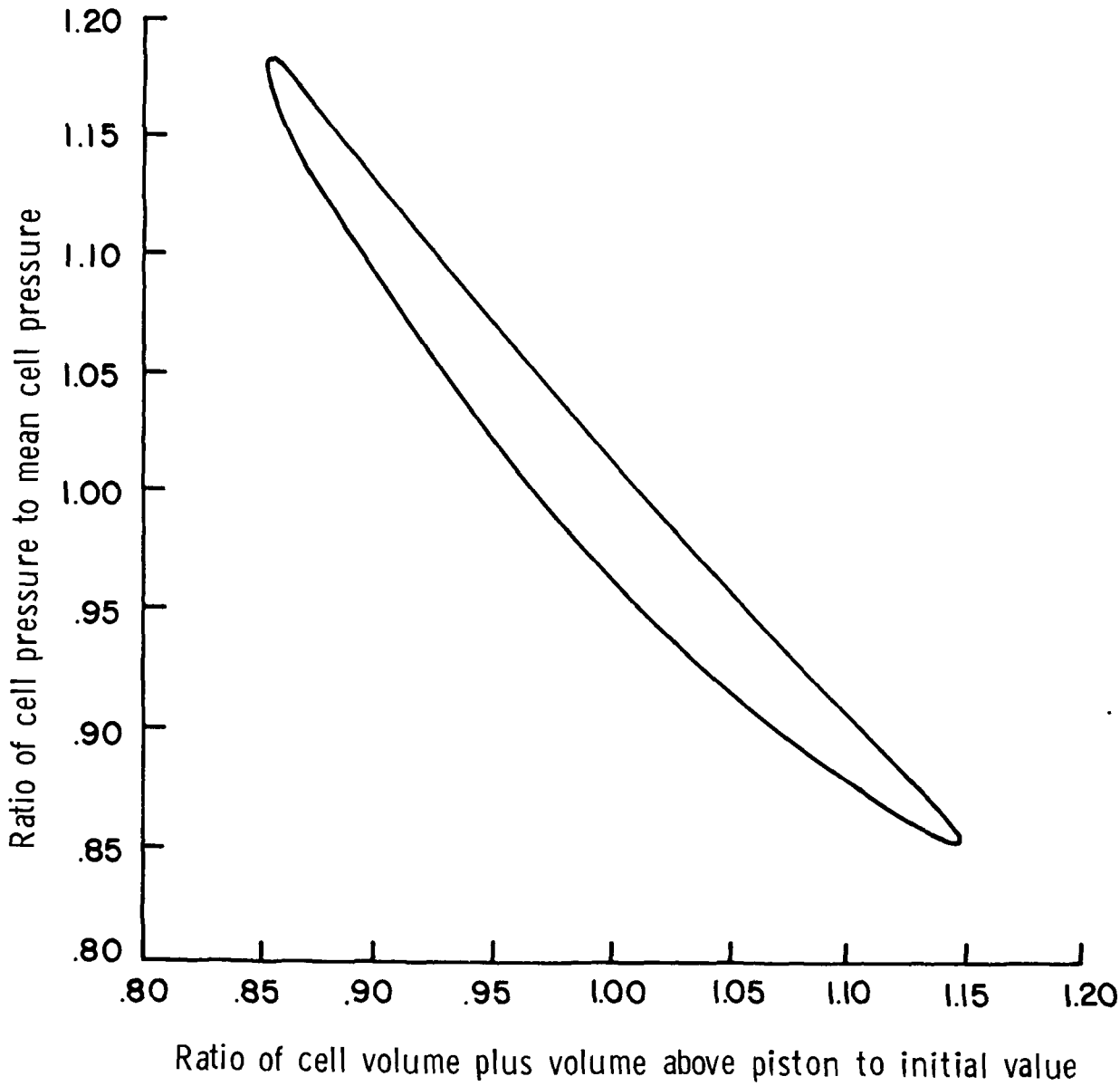

Figure 5.- Relative cell pressure vs. relative cell volume for 1-cm long cell with mean cell pressure of 6.67 kPa (66.7 mbar).

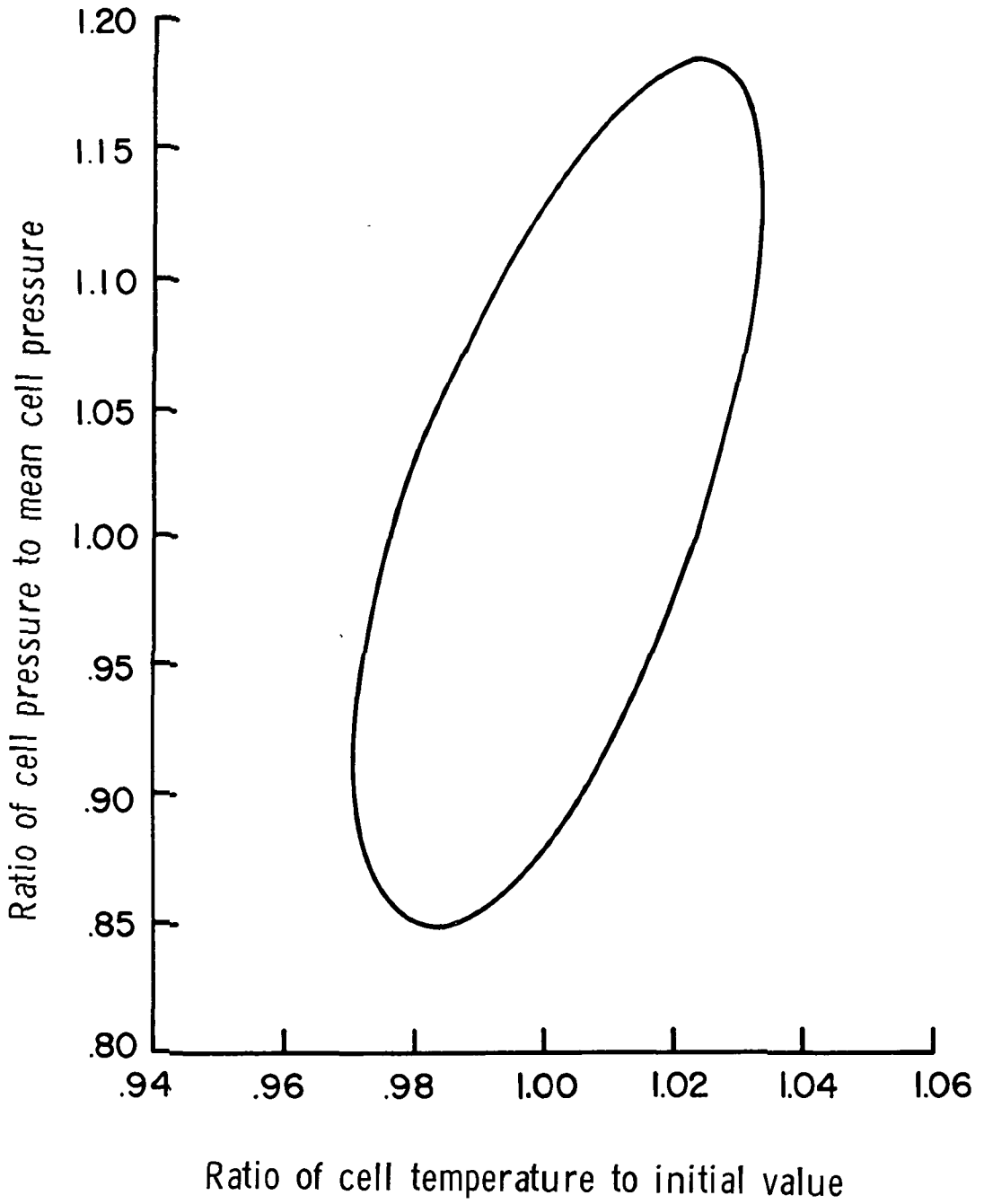

Figure 6.- Relative cell pressure vs. relative cell temperature for 1-cm long cell with mean cell pressure of 6.67 kPa (66.7 mbar).

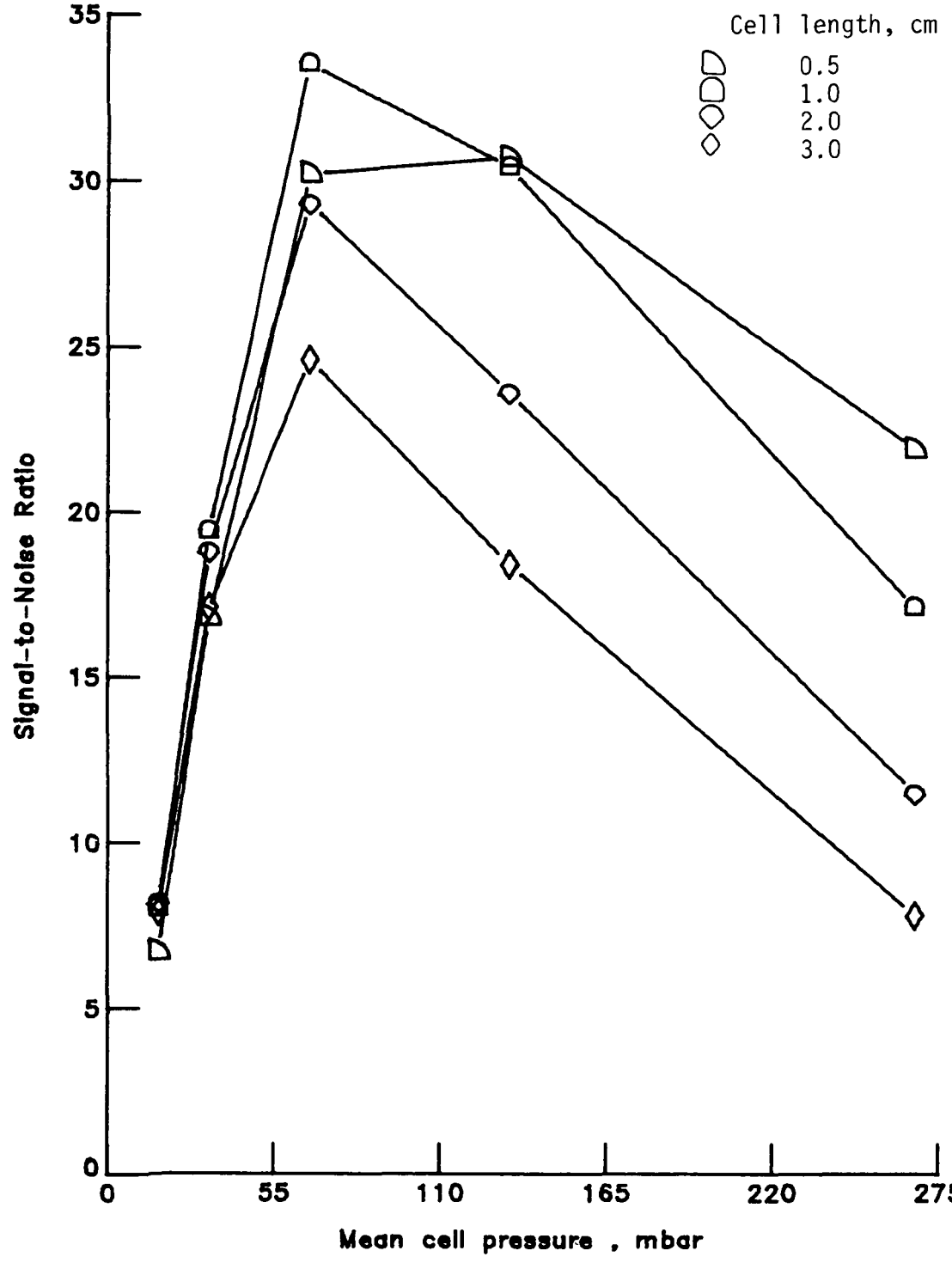

Figure 7.- Signal-to-noise ratio of 10-percent change in CO mean mixing ratio for different cell lengths.

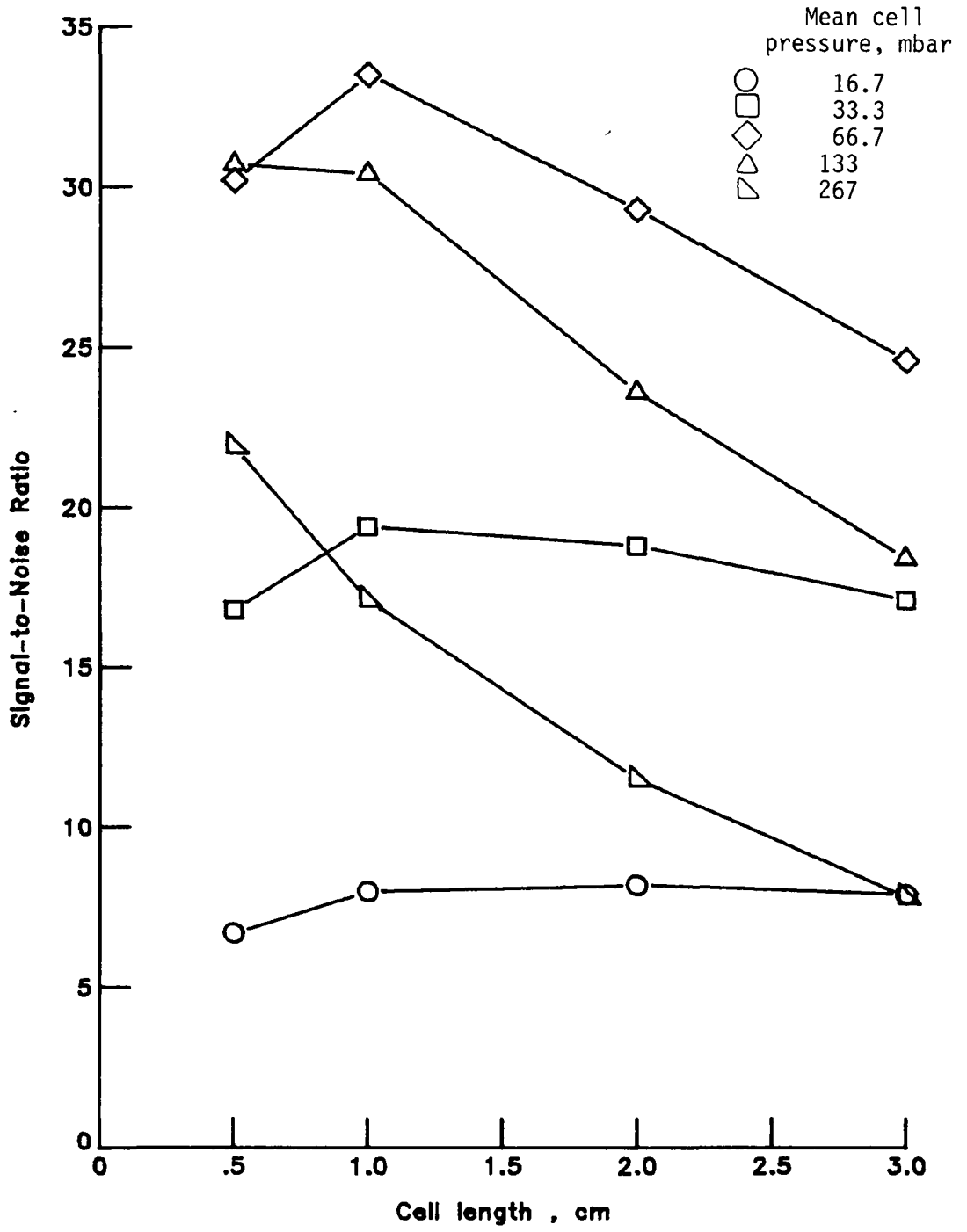

Figure 8.- Signal-to-noise ratio of 10-percent change in CO mean mixing ratio for different mean cell pressures.

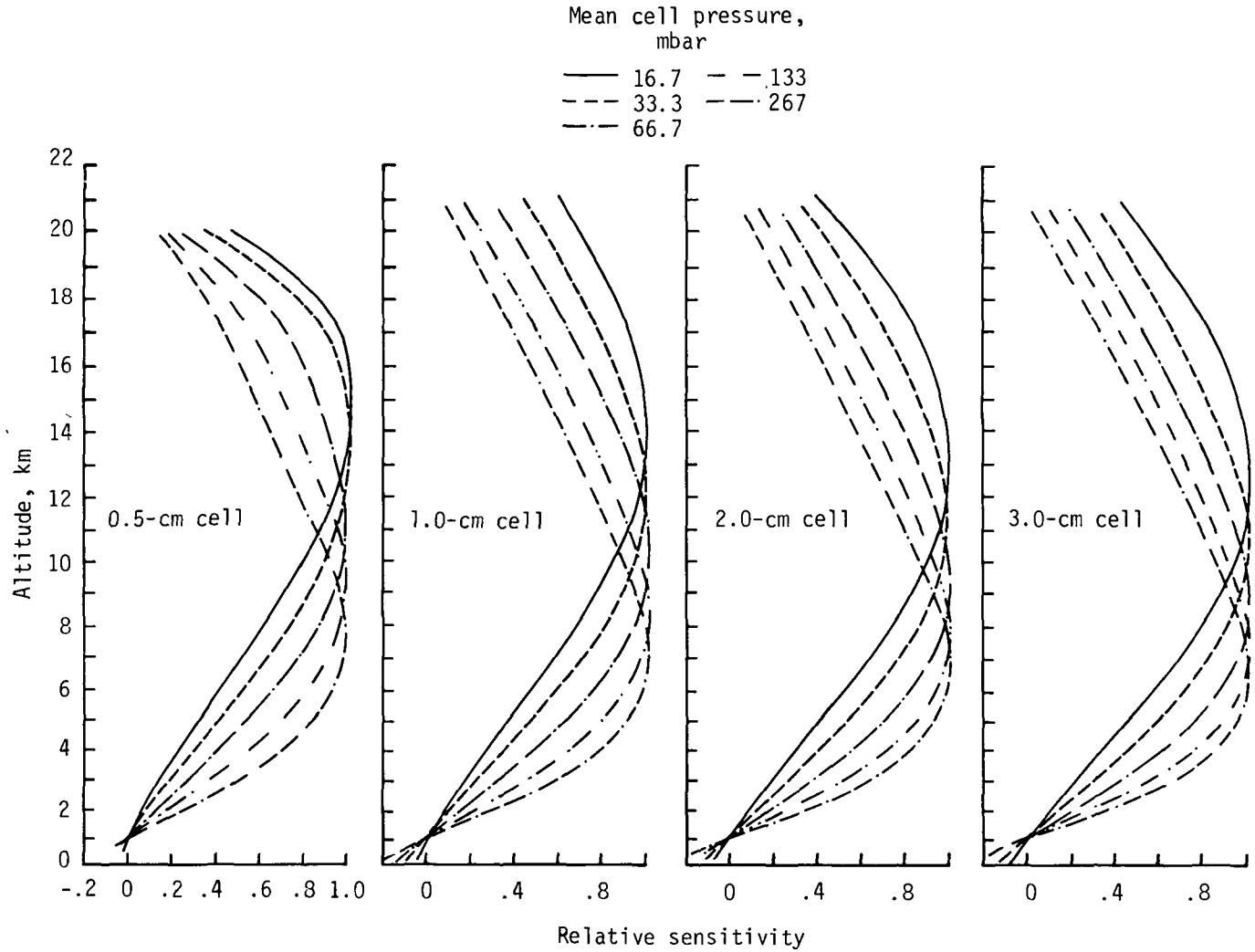

Figure 9.- Variation with altitude of PMR sensitivity to change of CO mixing ratio in single layer of mid-latitude summer model of atmosphere, with CO the only infrared-active species, (see eq. (11)). Maximum of each curve is normalized to 1.

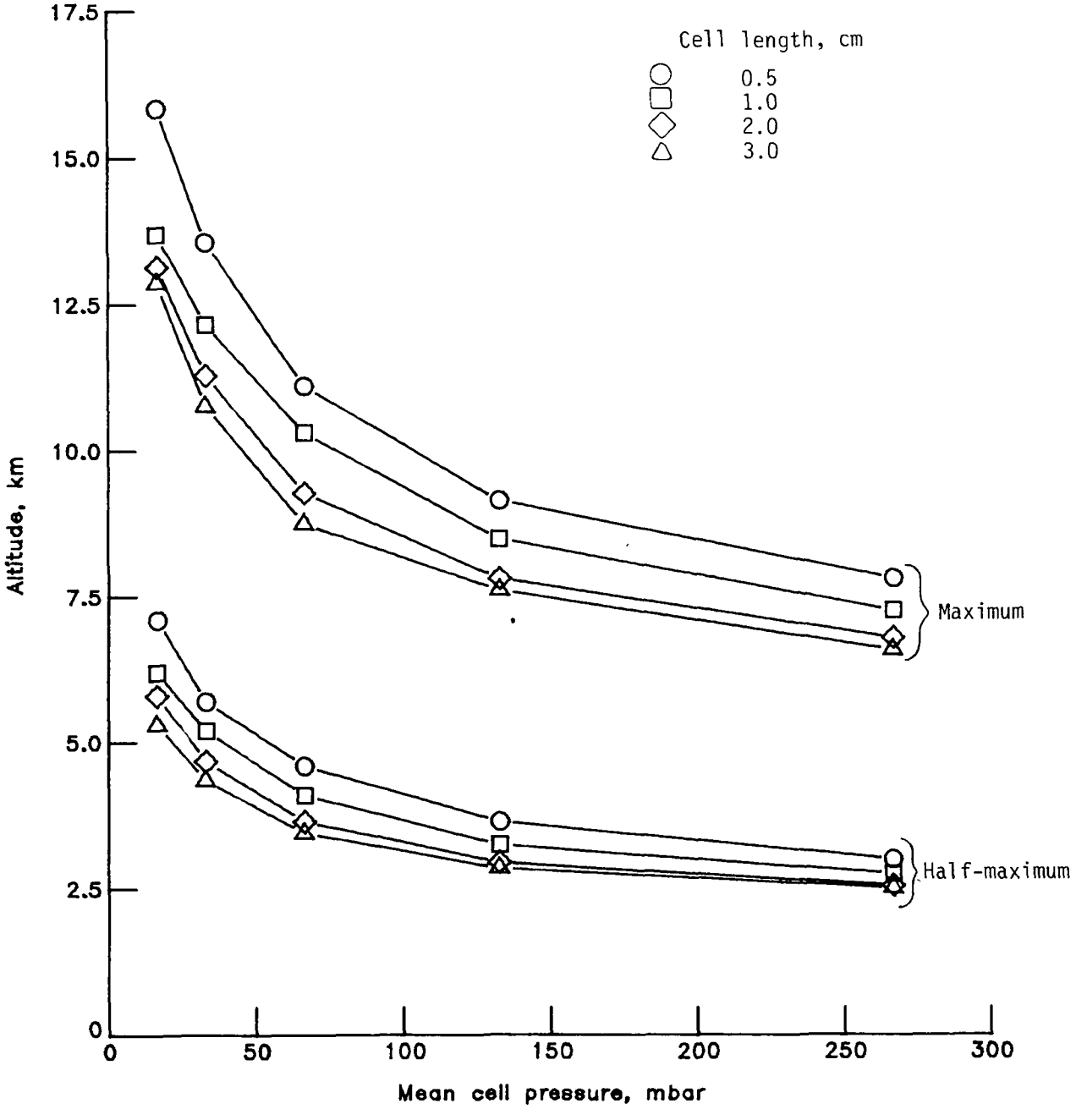

Figure 10.- Altitudes of maxima and half-maxima of VSD function vs. mean cell pressure.

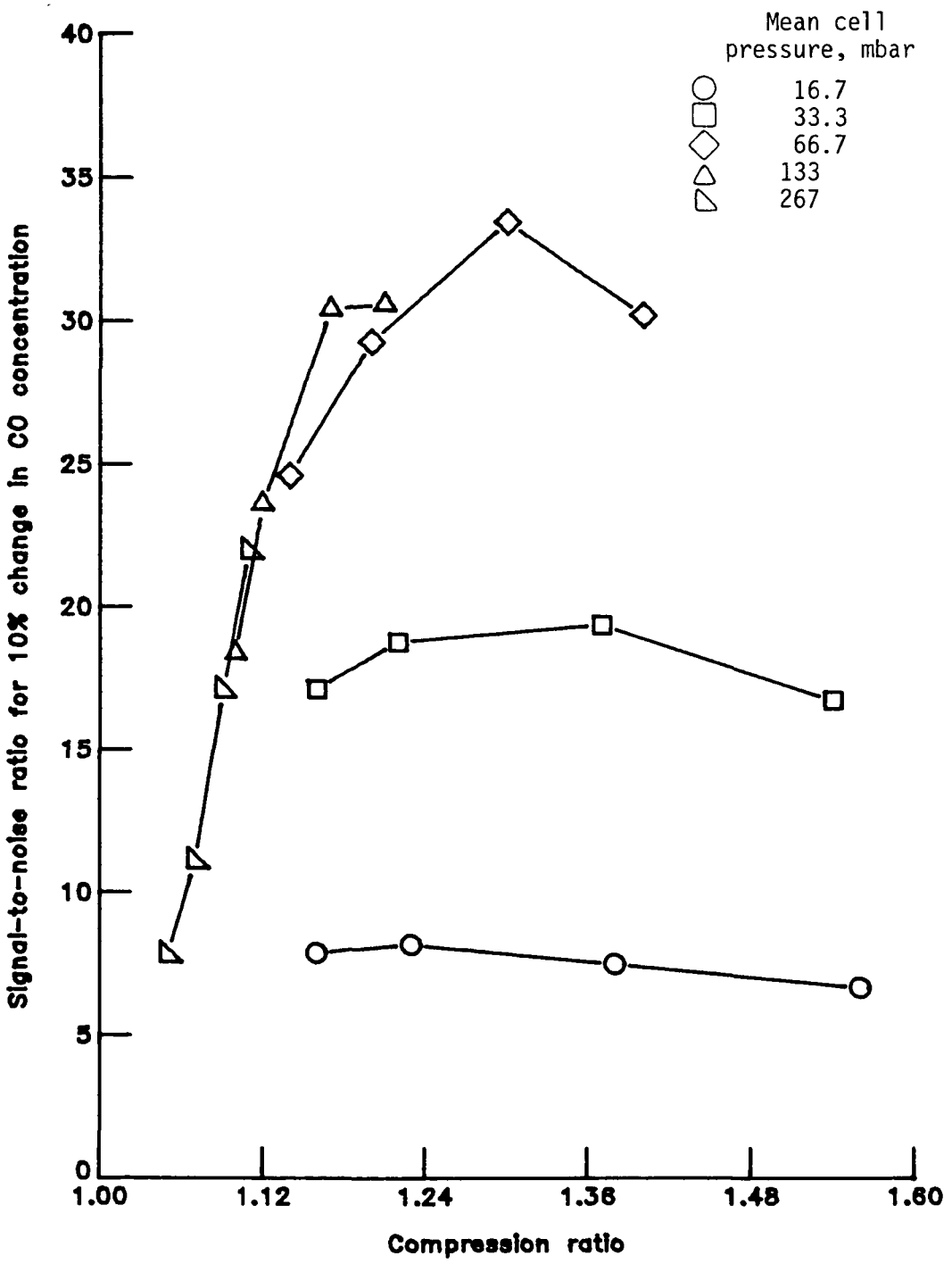

Figure 11.- Signal-to-noise ratio for 10-percent change in CO concentration vs. compression ratio.

1 Report No	2. Government Accession No	3 Recipient's Catalog No
NASA TM-81958		

4 Title and Subtitle	5 Report Date
PRELIMINARY FEASIBILITY ANALYSIS OF A PRESSURE MODULATOR RADIOMETER FOR REMOTE SENSING OF TROPOSPHERIC CONSTITUENTS	April 1981
	6 Performing Organization Code 146-20-10-13
7 Author(s)	8 Performing Organization Report No
Harry D. Orr III and Pamela L. Rarig	L-14094
	10 Work Unit No
9 Performing Organization Name and Address	
NASA Langley Research Center Hampton, VA 23665	11 Contract or Grant No
	13 Type of Report and Period Covered
12 Sponsoring Agency Name and Address	Technical Memorandum
National Aeronautics and Space Administration Washington, DC 20546	14 Sponsoring Agency Code

15 Supplementary Notes

Harry D. Orr III: Langley Research Center, Hampton, Virginia.
Pamela L. Rarig: Systems and Applied Sciences Corp., Hampton, Virginia.

16 Abstract

A pressure modulator radiometer operated in a nadir-viewing mode from the top of a mid-latitude summer model of the atmosphere was theoretically studied for monitoring the mean volumetric mixing ratio of carbon monoxide in the troposphere. The mechanical characteristics of the instrument on the Nimbus 7 Stratospheric and Mesospheric Sounder experiment are assumed and CO is assumed to be the only infrared active constituent. A line-by-line radiative transfer computer program is used to simulate the upwelling radiation reaching the top of the atmosphere. The performance of the instrument is examined as a function of the mean pressure in and the length of the instrument gas correlation cell. Instrument sensitivity is described in terms of signal-to-noise ratio for a 10-percent change in CO mixing ratio. Sensitivity to mixing ratio changes is also studied. It is concluded that tropospheric monitoring requires a pressure modulator drive having a larger swept volume and producing higher compression ratios at higher mean cell pressures than the Nimbus 7 design.

17 Key Words (Suggested by Author(s))	18. Distribution Statement
Remote sensing Tropospheric gases Radiometer, pressure modulator Gas correlation technique	Unclassified - Unlimited Subject Category 35

19 Security Classif (of this report)	20 Security Classif (of this page)	21 No of Pages	22 Price
Unclassified	Unclassified	28	A03

For sale by the National Technical Information Service, Springfield, Virginia 22161

NASA-Langley, 1981